

REPORT DOCUMENTATION PAGE			Form Approved OMB NO. 0704-0188	
Public reporting burden for this collection of information is estimated to average 1 hour per response, including the time for reviewing instructions, searching existing data sources, gathering and maintaining the data needed, and completing and reviewing the collection of information. Send comment regarding this burden estimate or any other aspect of this collection of information, including suggestions for reducing this burden, to Washington Headquarters Services, Directorate for Information Operations and Reports, 1215 Jefferson Davis Highway, Suite 1204, Arlington, VA 22202-4302, and to the Office of Management and Budget, Paperwork Reduction Project (0704-0188), Washington, DC 20503.				
1. AGENCY USE ONLY (Leave blank)	2. REPORT DATE 3/13/00	3. REPORT TYPE AND DATES COVERED Final Report, 1/96-12/17/99		
4. TITLE AND SUBTITLE Real-Time X-ray Scattering Study of Processing of Thermoplastic Polymers: Effects of Stress			5. FUNDING NUMBERS DAAH04-96-1-0009	
6. AUTHOR(S) Prof. Peggy Cebe				
7. PERFORMING ORGANIZATION NAMES(S) AND ADDRESS(ES) Tufts University STC-208, 4 Colby Street Medford, MA 02155			8. PERFORMING ORGANIZATION REPORT NUMBER 042-103-634/11397	
9. SPONSORING / MONITORING AGENCY NAME(S) AND ADDRESS(ES) U.S. Army Research Office P.O. Box 12211 Research Triangle Park, NC 27709-2211			10. SPONSORING / MONITORING AGENCY REPORT NUMBER ARO 35027.5-M5	
11. SUPPLEMENTARY NOTES The views, opinions and/or findings contained in this report are those of the author(s) and should not be construed as an official Department of the Army position, policy or decision, unless so designated by other documentation.				
12a. DISTRIBUTION / AVAILABILITY STATEMENT Approved for public release; distribution unlimited.			12 b. DISTRIBUTION CODE 20000707 155	
13. ABSTRACT (Maximum 200 words)  During the course of this research program we have contributed significantly to the understanding of structure/processing relationships in thermoplastic polymers crystallized from the melt. We concentrated efforts in metallocene-synthesized polyolefins, viz., polypropylene and polyethylene. Real-time wide and small angle X-ray scattering were performed to study the development of different crystallographic phases in PP and PE. Multiple crystallographic forms crystallize in PP, including the orthorhombic gamma and monoclinic alpha phases. Kinetics of crystallization were measured for each phase. We demonstrated that gamma crystallizes at higher temperature than alpha, but melts at lower temperature. Gamma does not convert into alpha upon heating. We showed that nucleation and growth is the mechanism of crystal formation (not spinodal decomposition, as suggested by others). Stress was incorporated into a study of effects of zone-drawing on the structure of PE. Structure was studied using molecular retraction, X-ray scattering and thermal analysis as functions of drawing stress and temperature.				
14. SUBJECT TERMS			15. NUMBER OF PAGES	
			16. PRICE CODE	
17. SECURITY CLASSIFICATION OR REPORT UNCLASSIFIED	18. SECURITY CLASSIFICATION OF THIS PAGE UNCLASSIFIED	19. SECURITY CLASSIFICATION OF ABSTRACT UNCLASSIFIED	20. LIMITATION OF ABSTRACT UL	

**FINAL REPORT - DAAH04-96-1-0009**

Professor Peggy Cebe  
Tufts University  
Department of Physics and Astronomy  
Science and Technology Center

Presented to Dr. Robert Reeber  
Army Research Office  
March 13, 2000

### Executive Summary of DAAH04-96-1-0009

Under this research program we have demonstrated the following structure-processing relationships, and effects of stress, in novel thermoplastic polyolefins:

1. We have been working in a novel Poly(propylene), synthesized by use of metal catalysts (so-called, metallocene isotactic poly(propylene), or m-iPP) which possesses low isotacticity and high defect chain structure. Unlike other types of iPP, this m-iPP crystallizes with multiple crystallographic forms, under ordinary processing conditions. We have shown that at elevated temperature, a large fraction of the crystallographic gamma phase crystallizes, up to 0.65 of the total crystal fraction. Using simultaneous real-time wide and small angle X-ray scattering we have for the first time measured separately the kinetics of the growth of alpha and gamma crystal phases in m-iPP.
2. Using the same techniques, we have shown for the first time that the orthorhombic gamma phase, while crystallizing at higher temperature, actually melts at lower temperature, than the monoclinic alpha phase m-iPP.
3. We have shown that the gamma phase does not recrystallize during heating, nor does it transform into the alpha phase, in contrast to earlier reports by other researchers. Each phase behaves separately, which is important for the ultimate morphology created during thermal processing, since the mechanical properties of these two phases are different.
4. In a subject currently of great interest, we have shown that the m-iPP in our study crystallizes by a *nucleation and growth* mechanism and not by spinodal decomposition as has been suggested by others.
5. We have observed the growth of dual low angle Bragg peaks for the first time using real-time small angle X-ray scattering. These peaks form in a sample crystallized so as to possess only one crystallographic phase (alpha). These two Bragg peaks are to be associated with different coherently scattering stacks of lamellar crystals caused by the unique cross-hatched structure in m-iPP.
6. In metallocene polyethylene, m-PE, we have performed zone-drawing for the first time, to study effects of stress on structure. Elongation during zone-drawing occurs by a mechanism of disruption of spherulite superstructure, facilitated by drawing at elevated temperatures.

## 1. INTRODUCTION

The purpose of this research program was to studying the effects of processing on the ultimate structure of thermoplastic polymers, incorporating the effects of stress. To this end, we applied the techniques of synchrotron X-ray scattering and differential scanning calorimetry to study several types of thermoplastic polymers. The project settled on a class of polymers of great current commercial and scientific interest: metallocene synthesized polyolefins, including polypropylene and polyethylene. These materials are newly available synthetic polymers created using transition metal single-site catalysts. The result of this new chemistry is a very uniform number of monomers (chemical building block for the polymer) in each polymer chain. The study of metallocene synthesized materials is one of the hottest research areas at present for the study of semicrystalline polymers, owing to the highly specific control over structure and properties that can be asserted by changing the polymer chain length and uniformity.

These materials were new for our research group, and we had to understand their particular thermal and structural properties that proved to be quite different from other thermoplastic polymers we used before. In particular, these polyolefins exhibit multiple crystallographic phases, multiple endothermic responses, and different response to stress application compared to conventionally synthesized materials. The crystallographic gamma phase in polypropylene (to be described more fully later on) is readily obtained in this material at ambient conditions. In contrast, in conventionally synthesized isotactic polypropylene (iPP), gamma phase is not observed except under very unusual conditions such as high-pressure crystallization. The importance of the gamma phase is that it is so far the only known example of a polymer in which the crystal chain stems are not parallel. Thus, we had available to us a unique opportunity to study the rarest of the crystallographic phases in iPP. In addition, recent questions have arisen about the fundamental nature of the crystallization process in iPP, whether by nucleation and growth, or by spinodal decomposition of the melt. The results of our research program are just beginning to be published, and will provide valuable insights into the structure and processing relationships for this new class of polymers.

This has been a very successful research program spanning the time just after my first arrival at Tufts to the present. The total time for the contract included the calendar years 1996-1999, with the latter year constituting a no-cost extension. Original start up at Tufts was slow due to the necessity of setting up our new laboratories, and attendant new equipment additions. A graduate student, Patrick Dai, began work on the project in June 1996, and spent the first year acquiring the skills needed for sample preparation, literature review, thermal properties measurement, theory and practice of X-ray scattering and diffraction, experimental protocol at Brookhaven synchrotron, and computer programming. Patrick began data collection in Year 1, and wrote first drafts of the computer algorithms for data analysis. We originally prepared several devices for injecting hot polymer into the X-ray beam at Brookhaven National Laboratory. However, the metallocene isotactic polypropylenes (m-iPP) were not understood from the standpoint of even relatively simple thermal processing, and much of Year 2 was spent in performing isothermal and non-isothermal crystallization studies. The injection devices were set aside while we concentrated on the relationship between dual melting behavior and structure. At this point we realized that *in-situ* wide angle X-ray scattering (WAXS) would be necessary in order to sort out the complex interplay between the different crystallographic phases. Year 3 produced our greatest accomplishment, bringing a new instrument on line providing us with the ability to perform real-time simultaneous wide and small angle X-ray scattering (SAXS) at Brookhaven. Finally, during our extension year, we attacked the problem of the nucleation mechanism for m-iPP. By using simultaneous WAXS and SAXS we demonstrated that m-iPP crystallizes by a nucleation and growth mechanism, and not spinodal decomposition, as proposed by others [Ryan].

At the same time, work was proceeding on the application of stress to a related material, metallocene-synthesized polyethylene. Undergraduate students Elizabeth Oyebode and David Berns prepared samples to study effects of zone-annealing/zone-drawing on the microstructure. Stress was applied at elevated temperatures in a narrowly heated zone, causing deformation of the polymer. Small angle X-ray scattering, differential scanning calorimetry, optical microscopy, and molecular retraction measurements were made on the m-PE. First publication of these results occurred in March 2000. In the next sections of the report, we go into more detail about the

publications, personnel, and specific findings of our research.

## 2. PUBLICATIONS AND PRESENTATIONS UNDER DAAH04-96-1-0009

### 1. List of Manuscripts Published, Submitted or in Preparation

This research program was a very productive one, with 2 papers already published, 5 papers in preparation, and 5 conference proceedings published. The research lead also to 13 scientific presentations, 10 of which were invited.

- [1] Patrick S. Dai, Peggy Cebe, Malcolm Capel, Rufina Alamo, and Leo Mandelkern. "Simultaneous *In-situ* WAXS and SAXS Study of Crystallization and Melting Behavior of Metallocene Isotactic Poly(propylene)." in *Scattering from Polymers: Characterization by X-rays, Neutrons, and Light* (Eds: P. Cebe, B. Hsiao, D. Lohse) ACS Symposium Series 739 (2000) 152-165.
- [2] Patrick S. Dai, Peggy Cebe, Malcolm Capel, Rufina Alamo, and Leo Mandelkern. "Small and Wide Angle X-ray Scattering Study of Metallocene Isotactic Poly(propylene)." *J. Applied Crystallography*, in press for 2000.
- [3] Patrick S. Dai, Peggy Cebe, Rufina Alamo, and Leo Mandelkern. "Study of Metallocene Isotactic Poly(propylene) Prepared by Partial Melting: I. Thermal Analysis." in preparation for *J. Polymer Sci., Phys. Ed.*, 3/00.
- [4] Patrick S. Dai, Peggy Cebe, Malcolm Capel, Rufina Alamo, and Leo Mandelkern. "Study of Metallocene Isotactic Poly(propylene) Prepared by Partial Melting: II. Wide and Small Angle X-ray Scattering." in preparation for *J. Polymer Sci., Phys. Ed.*, 3/00.
- [5] Patrick S. Dai, Peggy Cebe, Malcolm Capel, Rufina Alamo, and Leo Mandelkern. "Real-Time wide and Small Angle X-ray Scattering Study of Melting Kinetics in Metallocene Isotactic Poly(propylene)." in preparation for *Polymer*, 4/00.
- [6] Peggy Cebe, Andrew MacLennan, Jeremy Stern and Elizabeth Oyeboode. "Development of the Glass Transition in Poly(ethylene sulfide) Cold Crystallized at Low Temperatures." in preparation for *Macromolecules*, 5/00.
- [7] David Berns, Benita Dair, Elizabeth Oyeboode, Peggy Cebe, and Malcolm Capel. "Zone-Drawing of Metallocene Polypropylene." in preparation for *Polymer*, 5/00.
- [8] Patrick S. Dai, Peggy Cebe, Rufina Alamo, and Leo Mandelkern. "Crystallization and Melting of Narrow Molecular Weight Distribution Poly(propylene) Prepared

- by Partial Melting." *American Chemical Society, Proceedings of the Division of Polymeric Materials: Science and Engineering*, 78, 217 (1998).
- [9] Patrick S. Dai, Peggy Cebe, Rufina Alamo, Leo Mandelkern, and Malcolm Capel. "Real-Time SAXS Study of Crystallization of Metallocene Poly(propylene)." *American Chemical Society, Proceedings of the Division of Polymeric Materials: Science and Engineering*, 79, 322 (1998).
- [10] Peggy Cebe, Elizabeth Oyebode, and Lan Luo. "The Polymer Glass Transition: From Amorphous to Semicrystalline Polymers." *American Chemical Society, Proceedings of the Division of Polymeric Materials: Science and Engineering*, 80, 287 (1999).
- [11] Patrick S. Dai, Peggy Cebe, Rufina Alamo, and Leo Mandelkern "Self-Nucleation Study of Metallocene Isotactic Poly(propylene)." *American Chemical Society, Proceedings of the Division of Polymeric Materials: Science and Engineering*, 81, 264 (1999).
- [12] David Berns, Elizabeth Oyebode and Peggy Cebe. "Zone Drawing of Metallocene Polyethylene." *American Chemical Society, Proceedings of the Division of Polymeric Materials: Science and Engineering*, 82, 66 (2000).

## 2. Papers Presented

May 1997, "Creation and Relaxation of Constraints on Amorphous Phase Mobility." Seminar, Eastman Kodak Company, Rochester, NY. (invited)

May 1997, "Creation and Relaxation of Constraints on Amorphous Phase Mobility." Seminar, EXXON Research Corporation, Annandale, NJ. (invited)

September 1997, "Modulated Differential Scanning Calorimetry Study of Polymers with Constrained Amorphous Phases" New England Thermal Analysis Society, Waltham, MA. (invited)

January 1998, "Modulated Differential Scanning Calorimetry Applied to the Study of Semicrystalline Polymers" Seminar, Raytheon Corp. , Waltham, MA. (invited)

March 1998, "Thermal Analysis and X-ray Scattering Study of Two-Stage Melt Crystallization of PEEK," ACS National Meeting, Dallas.

March 1998, "Real-Time SAXS Study of Crystallization of Metallocene Poly(propylene)," ACS National Meeting, Dallas.

June 1998, "Modulated Differential Scanning Calorimetry And X-ray Analysis of Crystallization Near Tg," V<sup>th</sup> Lahnwitzseminar on Calorimetry Kuhlungsborn, Germany. (invited)

June 1998, "Relaxation of Liquid Crystal Alignment Layers - A Technique for Assessing the Glass Transition of Thin Polymer Films." University Catholique de Louvain, Seminar, Louvain-la-Neuve, Belgium. (invited)

June 1998, "Structural Studies of Semicrystalline Polymers and Blends Using Synchrotron Radiation." Imperial College of Science, Technology and Medicine, Seminar, London. (invited)

March 1999, "The Polymer Glass Transition: From Amorphous to Semicrystalline Polymers." American Chemical Society, Symposium on 75 Years of Advances in Applied Polymer Science, Anaheim, CA. (invited)

April 1999, "The Polymer Glass Transition: From Amorphous to Semicrystalline Polymers." American Chemical Society, Symposium on 75 Years of Advances in Applied Polymer Science, Anaheim, CA. (invited)

August 1999, "SAXS Study of Crystallization of Metallocene Isotactic Poly(propylene) Prepared by Partial Melting." American Chemical Society, Poster Session of the General Papers/New Concepts Symposium, New Orleans, LA.

April 2000, "Synchrotron X-ray Scattering Studies of Polymer Structure." Boston University Condensed Matter Physics Colloquium, Boston, MA. (invited)

### 3. SCIENTIFIC PERSONNEL SUPPORTED UNDER DAAH04-96-1-0009

Prof. Peggy Cebe	Supervisor	1/96-12/17/99
Dr. Benita Dair	Postdoctoral Research Assoc.	9/15/99-12/17/99.
Mr. Patrick S. Dai	Graduate Research Asst.	6/1/96-12/17/99 Ph. D. in Physics, to be awarded 5/00.
Ms. Elizabeth Oyebode	Undergraduate Asst.	6/96-6/99 (Balfour Scholarship for African American Students) B.S. in Physics, to be awarded 5/00
Mr. David Berns	Undergraduate Asst.	1/97-12/17/99 (Knight Prize in Physics; Nominated for Victor Prather Prize for Undergraduate Research, 2/2000) B.S. in Physics, to be awarded 5/00
Ms. Sarah Dubner	Undergraduate Asst.	1/97-12/17/99 (Howard Sample Prize in Physics; Knight Prize in Physics; Nominated for Tufts University Brown

Prize for Promise in Undergraduate Research,  
2/2000.) B.S. in Physics, to be awarded 5/00

## 4. SCIENTIFIC PROGRESS AND ACCOMPLISHMENTS

### 4.1 Experimental Considerations

#### 4.1.1 Materials

Poly(propylene) synthesized using metallocene catalyst is the subject of our study. This important, and still relatively new, synthetic route creates polymers with narrow molecular weight distribution. The phase structure and crystallization kinetics of the material depends upon defect content within the chain structure of the polymer. We are working with a novel high-defect content polymer that contains a large fraction of the gamma crystallographic phase. The relevance of the gamma phase of iPP is that it is “the first and so far unique example of a polymer structure with non-parallel chain stems.” [Lotz] (emphasis added). We have been studying the crystallization kinetics and melting behavior of samples of mixed crystal content. All other work in gamma phase iPP involves use of high-pressure conditions, or degradation of the molecular weight. Here, we are able for the first time to study gamma phase kinetics at ambient pressure, in un-degraded material.

The metallocene isotactic poly(propylene) (m-iPP) is an experimental product of Hoechst. Compared to conventional Ziegler-Natta type iPP, the m-iPP used in this study has a lower crystallization temperature and lower melting temperature. Characterization of the material [Alamo] shows that the fractional content of isotactic pentads (mmmm) is low at 0.908 mol-%, the  $M_w$  is 335,500 g/mol, and the polydispersity is 2.3. Stereo and regio defect contents are 1.68% and 0.67%, respectively.

#### 4.1.2 Techniques

Real-time *in-situ* SAXS and WAXS were performed at beam line X12B of the National Synchrotron Light Source at Brookhaven National Laboratory. The m-iPP sample, enclosed in two layers of Kapton<sup>TM</sup> tape, was located inside a Mettler FP82 hot stage. The m-iPP was first melted at 200°C for 1min, and then cooled at 10°C/min to

124.5°C (or 117°C) for isothermal crystallization for 3h (or 1h). For comparison, several longer crystallizations, up to 72h at 124.5°C, were carried out in a temperature regulated oil bath. The final melting endotherms were obtained by heating the sample from room temperature to 180°C at 1 or 5°C/min. Differential scanning calorimetric data were also obtained [Dai], using the modulated differential scanning calorimeter purchased under this contract.

SAXS data were collected with a two-dimensional position sensitive histogramming detector, with sample-to-detector distance of 180.0cm. Monochromatic X-radiation with a wavelength of 1.54Å was used. Data were taken continuously during the experiment, and each scan was of 60s duration. To improve the signal to noise ratio, several scans were binned together during data processing. Raw intensity was corrected for fluctuations in incident beam intensity, background, and sample absorption. The SAXS invariant,  $Q$ , was calculated from the Lorentz corrected intensity,  $I_s^2$ , using:

$$Q = \int_0^{\infty} I(s)s^2 ds \quad (1)$$

WAXS data were collected with a Braun 7cm one-dimensional position sensitive wire detector operated at 3KV, with the Argon/Methane (90/10) gas flowing at 1ml/min. Scans were collected for 60s, simultaneously with SAXS, over a  $2\theta$  angular range 10°-44°. D-spacings were calibrated by reference to NaCl and KCl powders.

In the WAXS diffractograms of iPP, many peaks of the  $\alpha$  and  $\gamma$  phase are in similar  $2\theta$  locations [Mezghani]. However, each modification has a distinctive reflection peak, which is well defined in our experiment. The  $\alpha$  and  $\gamma$  phases are distinguished by their own characteristic scattering angle  $2\theta$  and Miller indices (hkl), at 18.5° (130) for  $\alpha$ , and 20.2° (117) for  $\gamma$ . To quantify the relative amount of  $\alpha$  and  $\gamma$  crystals, we calculate the area,  $S(i)$  ( $i=1,2$  for  $\alpha$ ,  $\gamma$ , respectively) under the  $i^{\text{th}}$  WAXS peak after subtraction of the amorphous halo. The area ratio,  $\eta$ , is defined as:

$$\eta(i) = \frac{S(i)}{S(1) + S(2)} \quad (2)$$

and reflects the relative proportion of the  $i^{\text{th}}$  crystal phase.

For the application of stress, we used a zone-drawing apparatus that has been described previously [Aihara], and follows the slotted heater design of Garrett and Grubb [Garrett]. A heating element at constant temperature,  $T_d$ , passed over the sample, with one surface in contact with the sample, at a constant speed of approximately 2mm/s. At the same time a force was applied to the sample by means of a free weight.

The material studied was Exceed 350D60, a commercial metallocene PE produced by Exxon. For this material, Exxon reports a melt flow index of 1.0, with  $M_n = 43,390$  and  $M_w = 112,600$  [Bamberger]. The material was received in pellet form, then compression molded at 200°C into thin sheets, and quenched with cold water. The samples used for drawing were cut into strips 0.635 cm wide, with a thickness of 150-300 microns. The sample length was not critical and was typically about 3 cm.

The experiments consisted of drawing in the rubbery regime at 50°C, 60°C, 70°C, 80°C, 90°C, or 100°C. The maximum stress that could be applied to the samples was limited by the apparatus, which could only support masses of up to 2200g. Samples were characterized by three parameters: drawing temperature  $T_d$ , engineering stress,  $\sigma$ , and draw ratio,  $\lambda$ . Engineering stress is the ratio of the free weight to the initial cross sectional area of the sample. Draw ratio is defined as  $\lambda = (\text{final length})/(\text{initial length})$ . Elongation of the samples was measured using gold fiduciary marks deposited on the sheets by thermal evaporation through a copper mesh with a very fine and well-known spacing.

## 4.2 Results and Discussion

### 4.2.1 Real-Time X-ray Scattering of Metallocene-iPP

Poly(propylene) exists in several crystallographic phases. Alpha (monoclinic) and gamma (orthorhombic) phases have unique crystallographic reflections at  $2\theta$  scattering angle with Miller Indices (hkl), at 18.5° (130) for alpha, and 20.2° (117) for gamma. **Figure 1** shows WAXS intensity vs.  $2\theta$  during the first eight minutes of crystallization at 117°C. The distinctive alpha and gamma phase peaks are marked with arrows. We found at 117°C, alpha and gamma grow nearly simultaneously. Both types of crystals begin to grow within the first 2 minutes. Then follows the rapid growth of gamma crystals. By

the end of 4 minutes, the gamma peak is nearly as high as alpha peak, and by the end of 5 minutes, the gamma peak becomes even higher than the alpha peak. At the initial stage, the amount of alpha crystals is significantly larger than the gamma crystals. As time goes on, the gamma crystals catch up, and eventually form an even larger amount of crystals. This is the first time that crystallization of gamma phase has been observed in real-time.

During thermal analysis, upon directly heating from the crystallization temperature, we observe dual endotherms. We have been able to associate the lower melting endotherm to melting of gamma phase, and the upper melting endotherm to melting of alpha phase. **Figure 2** shows WAXS intensity vs. temperature during heating from 121°C to 140°C, which encompasses the lower melting DSC peak. After isothermal crystallization at 117°C for 60 minutes, we quenched the m-iPP sample to room temperature, and then heated at 1°C/min from 100°C to 170°C. The gamma crystals scattering intensity begins to drop at about 124°C, and this trend continues until finally gamma completely disappeared by 140°C. The intensity of alpha crystals remains nearly constant within this temperature range. These results show that gamma phase m-iPP does not recrystallize during DSC scanning, nor does it transform into alpha phase. Each phase appears to behave separately, which has important implications for the morphology created during thermal processing.

**Figure 3** is a sequence of WAXS curves taken during crystallization at 124.5°C. Each curve represents an average of four one-minute data collection scans. The binning of several scans causes some loss of time resolution, but was necessary in the earliest scans because of the very low crystal content and low perfection of crystals. From bottom to top the curves are : a.) 1-4min., amorphous; b.) 5-8min, imperfect crystals forming; c.) 13-16min.; d.) 21-24min.; e.) 29-32 min.; and, f.) 37-40min. Characteristic reflections for  $\alpha$  and  $\gamma$  are marked with arrows. It is clear from these data that crystals have nucleated and are detectable by WAXS at least by curve b, i.e., in the interval 5-8 min. after the crystallization temperature was reached.

The crystals forming early on are imperfect leading to variability in peak intensities and positions. When the crystallization time was increased to 3h, there were

systematic shifts to higher scattering angles in most of the major reflections. This suggests a continuous improvement in perfection in chain packing and densification of the unit cell structure, which will be reported more fully in a later publication. For crystallization at 117°C (not shown) WAXS results indicate that crystals are already nucleated within the second minute of isothermal holding. DSC melt crystallization kinetics at 117°C give an induction time of one minute [Dai].

**Figure 4** shows the relative time development of  $\alpha$  (solid squares) and  $\gamma$  (open circles) crystals from the areas beneath the characteristic WAXS peaks, for 124.5°C (**Figure 4a**) and 117°C (**Figure 4b**). Error bars on intensity are largest at early times due to the overall small size of the peaks. On the assumption that the scattering power is similar for  $\alpha$  and  $\gamma$ , these data suggest that  $\alpha$  and  $\gamma$  nucleate nearly simultaneously, but the ultimate fraction of  $\gamma$  crystals is greater than  $\alpha$  at these temperatures. At 124.5°C, if crystallization is prolonged beyond 3h, the amount of  $\alpha$  is barely changed while  $\gamma$  increases in agreement with prior work. The  $\gamma$  fraction from equation (3) rises from 0.67 after 3h to 0.8 after 72h. Additionally, at lower crystallization temperature, there is a greater the relative fraction of  $\alpha$  phase. These results agree with prior kinetics data from DSC and WAXS [Alamo; Dai].

**Figure 5** shows DSC heating scans taken after crystallization at 124.5°C and 117°C. Both data sets show two main melting endotherms, with  $\gamma$  and  $\alpha$  crystals melting primarily in the lower and upper endotherms, respectively [Alamo; Dai]. The broad shallow endotherm appearing at temperatures lower than the crystallization temperature arises from crystals formed during the cooling, and need not concern us here. Crystallization at 117°C results in a much sharper upper ( $\alpha$  phase melting) endotherm. Increasing to 124.5°C causes both main endotherms to shift to higher temperature compared to their positions after 117°C crystallization, and the  $\alpha$  melting endotherm becomes much smaller. At both temperatures, an increase in crystallization time causes the lower endotherm to increase in area, while the upper endotherm area is barely affected. This confirms the WAXS results showing an increase in  $\gamma$  crystal fraction with longer holding time, especially at 124.5°C.

**Figure 6** shows time development of SAXS intensity during crystallization at 124.5°C. Each time slice represents 60s of data collection. From the Lorentz corrected intensity vs. time data, we see that the Bragg peak intensity develops clearly by the fourteenth minute. The crystallization induction time can be better assessed from the SAXS invariant,  $Q$ , which from equation (1) is the area under the Lorentz corrected scattering curves in **Figure 6**. **Figure 7** shows  $Q$  vs. time during crystallization at 124.5°C (solid diamonds) and 117°C (open circles).  $Q$  becomes non-zero within the second minute of data collection at 117°C, and in the 14 min. interval at 124°C.

We also can verify that WAXS and SAXS are measuring the same overall kinetics, by comparing the half-times, or time for a characteristic parameter to reach its half-height value, found from each technique. At 124.5°C, the crystals develop fairly slowly, with a half time determined from  $Q$  in **Figure 7** of about  $t_{1/2} = 41-42\text{min}$ , in very good agreement with the WAXS data ( $t_{1/2} = 41-42\text{min}$ ) shown in **Figure 4**. At 117°C, the crystallization half-time from  $Q$  is between 3 and 4min (estimated at  $t_{1/2} = 3.5 \pm 0.5\text{min}$ ), in good agreement with WAXS (giving  $t_{1/2} = 4\text{min}$ ), and with DSC data showing maximum exothermic heat flow at 4min [Dai].

For isothermal crystallization at 117°C, the SAXS Bragg peak (**Figure 7**) appears nearly at the same time as the WAXS crystalline reflections. At 124.5°C, the SAXS Bragg peak appears several minutes after the WAXS crystalline reflections (**Figure 3**). These results support a nucleation and growth model for isothermal melt crystallization in this m-iPP that crystallizes to give a large fraction of the  $\gamma$  polymorph. Observation of SAXS intensity prior to WAXS intensity is thus not a universal feature for crystallization of iPP.

1. In this m-iPP,  $\alpha$  and  $\gamma$  crystals nucleate nearly simultaneously, and at the chosen crystallization temperatures, a greater amount of  $\gamma$  phase develops, up to 0.8 of the total crystalline fraction after long crystallization at 124.5°C.

2. The overall crystallization kinetics (relating to the half-time) is the same when determined by SAXS, WAXS, and DSC. Though these techniques measure different quantities, this result indicates that, roughly speaking, they are equally sensitive to the total crystallinity level, and its change with time.

3. At the earliest stages of crystal development, the SAXS Bragg intensity appears simultaneously, or slightly lags, the appearance of WAXS intensity, thus supporting a nucleation and growth model for this m-iPP. The multiple crystal phases observed in this m-iPP, and the ease of formation of the  $\gamma$  crystal phase, may play a role in the mechanism of crystal initiation and formation of long range ordered structures.

#### 4.2.2 Zone Drawing of Metallocene Polyethylene

Prior to drawing, samples of metallocene polyethylene were semi-crystalline with no preferred crystalline orientation, as confirmed by WAXS. DSC showed that different compression molded sheets had almost identical melting endotherm shapes and melting temperatures. Only one broad endothermic peak was seen, with maximum at about 114°C.

Samples were first characterized by their draw ratios. Figures 1 and 2 show typical plots of draw ratio vs. engineering stress for  $T_d = 60^\circ\text{C}$  and  $90^\circ\text{C}$ , respectively. From **Figure 8**, we see that drawing at a low temperature of  $60^\circ\text{C}$  (and also at  $T_d = 50^\circ\text{C}$ , which is not shown) results in very low draw ratios,  $\lambda = 1.1-1.3$  for engineering stresses in the range from 5 to 9 MPa. When the engineering stress was close to 9-10 MPa variable draw ratios were observed. An increase in draw ratio to  $\lambda = 2.7-4.0$  was seen in some samples while others did not draw significantly. For a stress of 15MPa, one sample drew to  $\lambda \sim 4.4$ . At low drawing temperatures of  $50^\circ\text{C}$  and  $60^\circ\text{C}$ , the samples did not achieve significant draw ratio until the stress exceeded about 10MPa, which is close to the reported yield stress of 8.4-8.8 MPa at room temperature [EXXON Product data sheet]. In **Figure 9**, we see that drawing at a high temperature of  $90^\circ\text{C}$  (and also at  $T_d = 70^\circ\text{C}$ ,  $80^\circ\text{C}$  and  $100^\circ\text{C}$ , which are not shown) results in a linear increase of draw ratio with engineering stress. Draw ratio ranges from 1.4-6.5 for engineering stresses from 3-13 MPa.

**Figure 10** is a plot of engineering stress vs.  $T_d$  for two draw ratios,  $\lambda = 3.4$  and  $\lambda = 4.5$ . Engineering stress decreases nearly linearly with drawing temperature, changing by about a factor of two from the lowest to the highest  $T_d$  at constant draw ratio. An increase in engineering stress at a constant drawing temperature results in an increase in

the draw ratio. Though the data are sparse, at low temperature it appears that a greater stress is required to achieve the increase in draw ratio from 3.4 to 4.5.

WAXS showed strong crystalline orientation in the drawn samples. However, no monoclinic crystal phase was identified in the zone-drawn samples. Only the reflections characteristic of the orthorhombic phase were seen [Wunderlich]. **Figure 11** shows a plot of the angular spread,  $\alpha$  (in degrees), of the WAXS equatorial reflections plotted as a function of  $T_d$ , for a constant  $\sigma$  of 11.6 MPa. At a constant engineering stress, an increase of  $T_d$  results in an increase in draw ratio, thus, the draw ratio increases in Figure 4 from 3.4 at 50°C to 5.9 at 80°C. The increase in draw ratio at constant stress results in a decrease in the angular spread of the reflections, indicative of higher orientational order of the crystallites. WAXS also showed that the crystallites become oriented (albeit to lesser extent) even when  $\lambda=1.1$ .

Molecular retraction experiments were conducted to assess the extension of the amorphous phase. Samples were cut to uniform lengths and heated to the melting point on a droplet of oil. The length after shrinkage was compared to the initial length. All samples showed substantial retraction (elastic recovery), verifying that the amorphous phase is extended, and not merely disentangled by chain slippage, during the drawing. Retraction data will be reported more fully in a subsequent manuscript.

Samples were examined using low magnification POM. At 50°C and 60°C on the low  $\lambda$  "plateau" (low stress region in **Figure 8**) we see a grainy pattern of birefringence indicative of large scale crystalline order, i.e., spherulites. However, at the high  $\lambda$  "plateau" at 50°C and 60°C (higher stress region in Figure 1), or for any  $\lambda$  at 70°C, 80°C, 90°C, or 100°C we do not see that grainy structure anymore even at the highest magnification. The samples appear uniformly birefringence, and no spherulite structure can be observed.

At low  $T_d$ , above a critical stress, similar phenomena as in the higher temperature data are observed. A natural thought is that the spherulites play the role of a barrier to elongation at low temperatures until a critical stress is reached. Initially, at low  $T_d$ , the lower modulus, interspherulitic amorphous phase extends and the sample elongates to low draw ratio. Stress is transferred to the higher modulus crystalline phase, until the

critical stress is reached, at which point elongation can proceed. We suggest elongation to higher draw ratio may proceed by disruption of the spherulitic superstructure, and this can occur at low  $T_d$  only by application of large stresses. Spherulite disruption is facilitated at high  $T_d$  and may therefore occur for all draw ratios.

### References

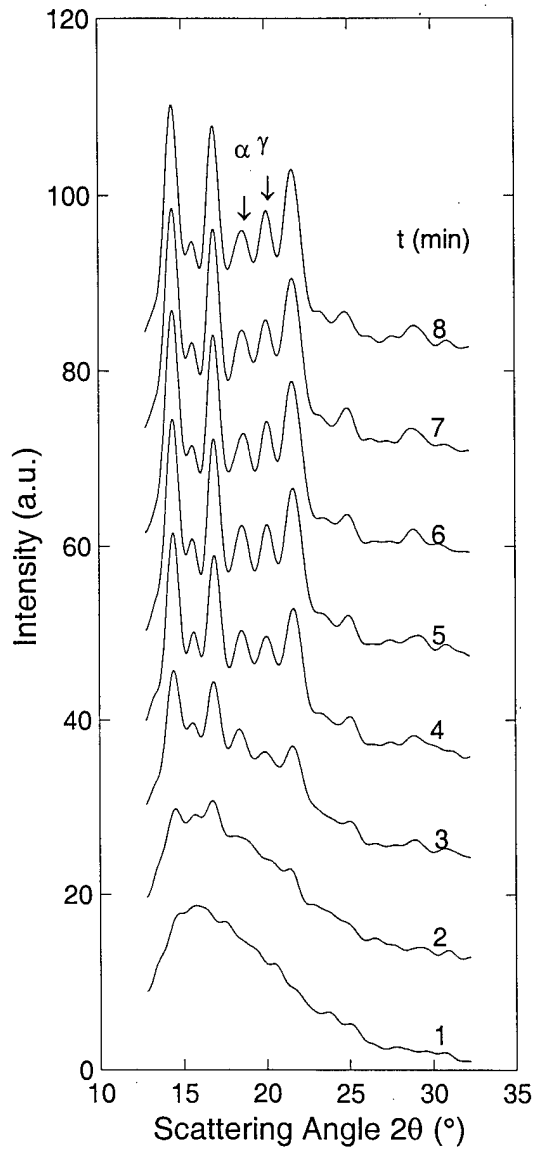
- Aihara, Y.; Cebe, P. *Polymer Engineering and Science*, **1994**, *34*(16), 1275.
- Garrett, P.; Grubb, D. T. *Polym. Comm.*, **1988**, *29*(3), 60.
- Dr. Robert Bamberger, private communication, 1997.
- Exxon Product Data Sheet, for EXCEED PE 350D60, 1999.
- Wunderlich, B. *Macromolecular Physics*, vol. 1, (Academic Press, NY, 1973) 97.
- Alamo, R. G., Galente, M. J., Lucas, J. C., Mandelkern, L. *Polym. Preprint.*, (1995). **36**, 285-286.
- Alamo, R. G., Kim, M. H., Galente, M. J., Isasi, J. R., & Mandelkern, L. (1999). To appear.
- Dai, P. S., Cebe, P., Capel, M., Alamo, R. G. & Mandelkern, L. (1999). *Scattering from Polymers;: Characterization by X-rays, Neutrons, and Light*, edited by P. Cebe, D. Lohse & B. Hsiao, ACS Symposium 739, 152 (2000).
- Lotz, B., Wittmann, J. C. & Lovinger, A. J. (1996). *Polymer*, **37**, 4979-4992.
- Mezghani, K. & Phillips, P. J. (1997). *Polymer*, **38**, 5725-5733.
- Ryan, A. J., Stanford, J. L., Bras, W. & Nye, T. M. W. (1997). *Polymer*, **38**, 759-768.

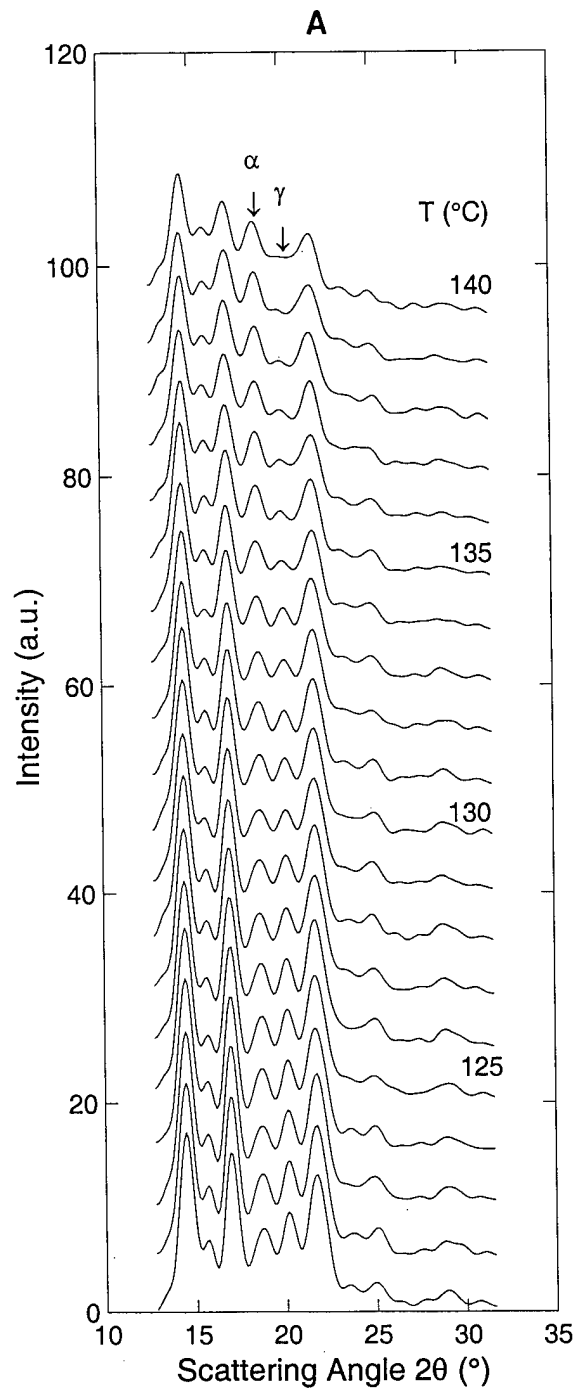
## Technology Transfer

I have been actively collaborating with two colleagues at Florida State University. **Prof. Rufina Alamo** is in the Chemical Engineering Dept. She is an expert in thermal analysis and structure of metallocene-based polymers, including polyethylene and polypropylene. **Prof. Leo Mandelkern** is in the Chemistry Department. He is a world expert in polyolefin structure, and is supplying the m-iPP used in our research. Both Alamo and Mandelkern are co-authors on our publications.

Several individuals and industries have approached me for assistance with X-ray and thermal analysis on their special polymers. I performed a project on real-time crystallization of polyolefins for **Dr. Alex Hsieh**, of the Army Research Laboratory at Aberdeen, MD. **Dr. Arnold Lustiger** of EXXON Corp. continues to be a source of non-metallocene polypropylene material, and we may engage in a joint research project on PP films this year. I have been able to assist **Dr. Ray Pariser**, of Marine Polymer Technologies, in the analysis of wide angle X-ray scattering patterns for a chitin-related material of interest to the Army. **Prof. Guiford Jones**, of Boston University Chemistry Department, approached me and is receiving assistance with thermal analysis on blended polymers of potential use for optical applications.

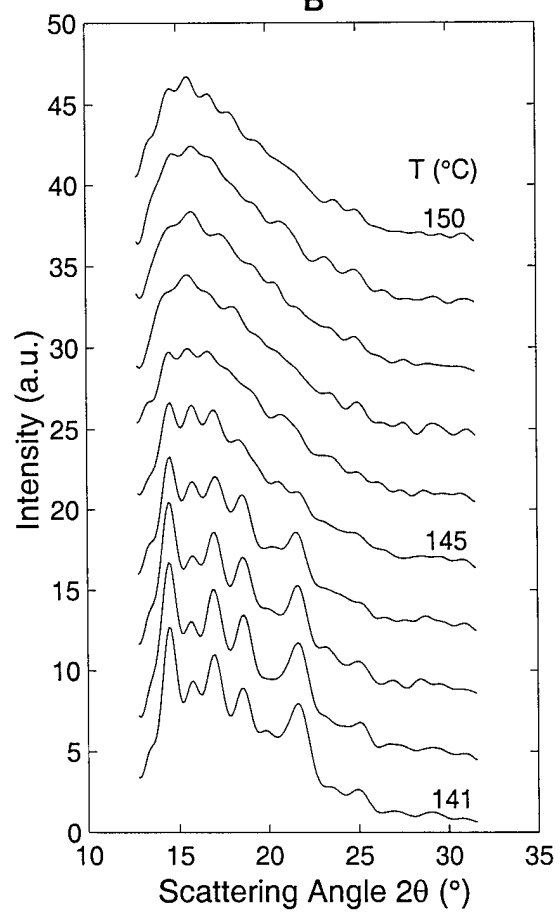
**Fig. 1** WAXS intensity vs. scattering angle,  $2\theta$ , during crystallization at  $117^\circ\text{C}$ , showing the development of alpha and gamma phase crystals.



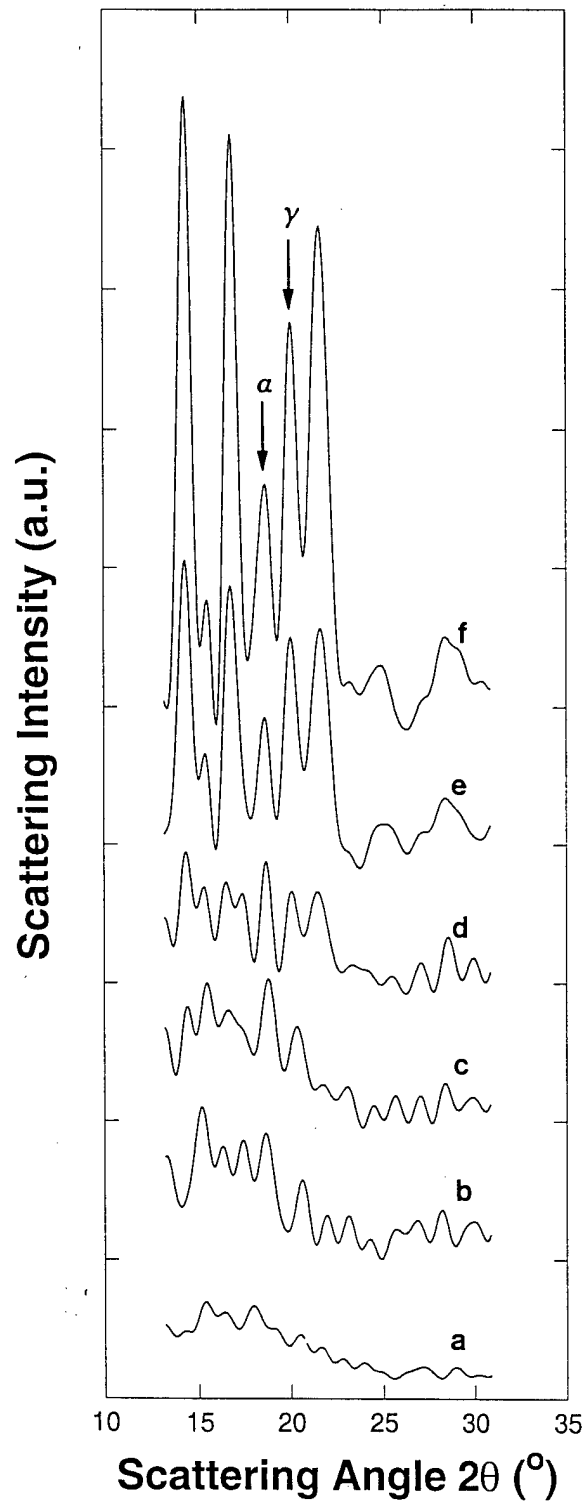


**Fig. 2** WAXS intensity vs. scattering angle,  $2\theta$ , during heating, showing melting of alpha and gamma phase crystals.

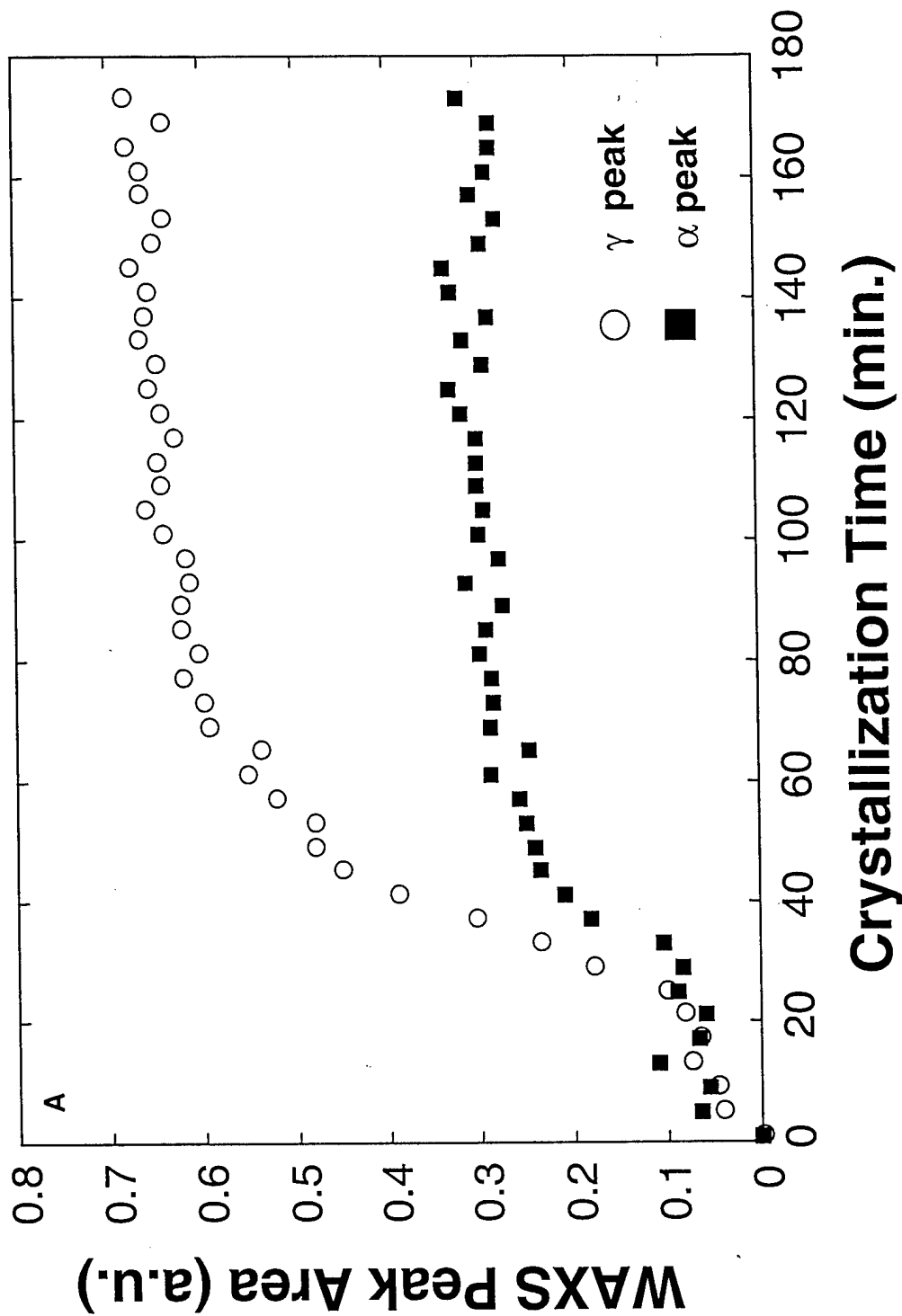
**B**

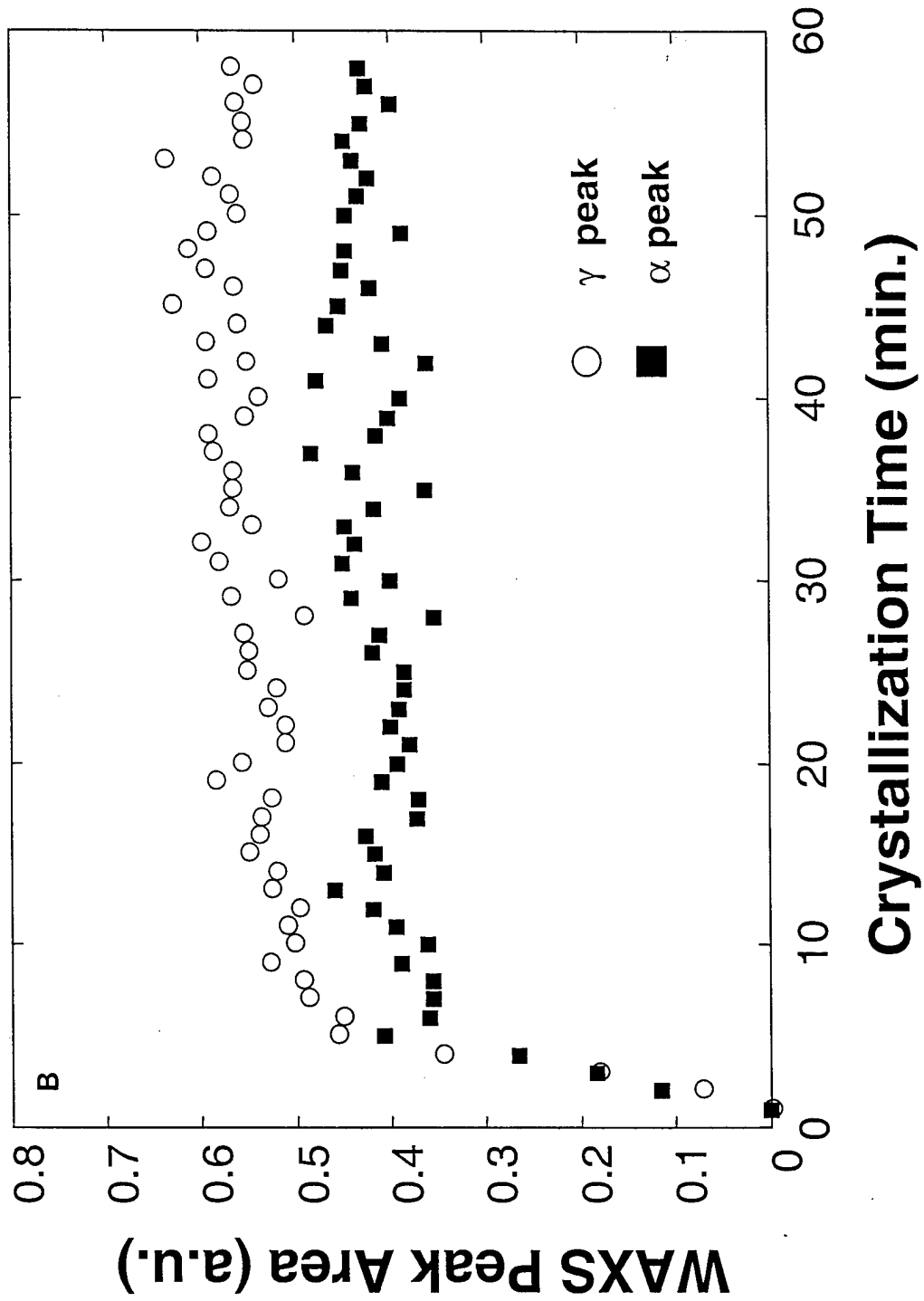


**Fig. 3** WAXS intensity of m-iPP vs. scattering angle,  $2\theta$ , at different times during isothermal crystallization at  $124.5^\circ\text{C}$ . Each curve is a time average of four one-minute scans. a.) 1-4min.; b.) 5-8min.; c.) 13-16min.; d.) 21-24min.; e.) 29-32 min.; and, f.) 37-40min. Characteristic peaks of  $\alpha$  and  $\gamma$  phases are indicated by arrows.

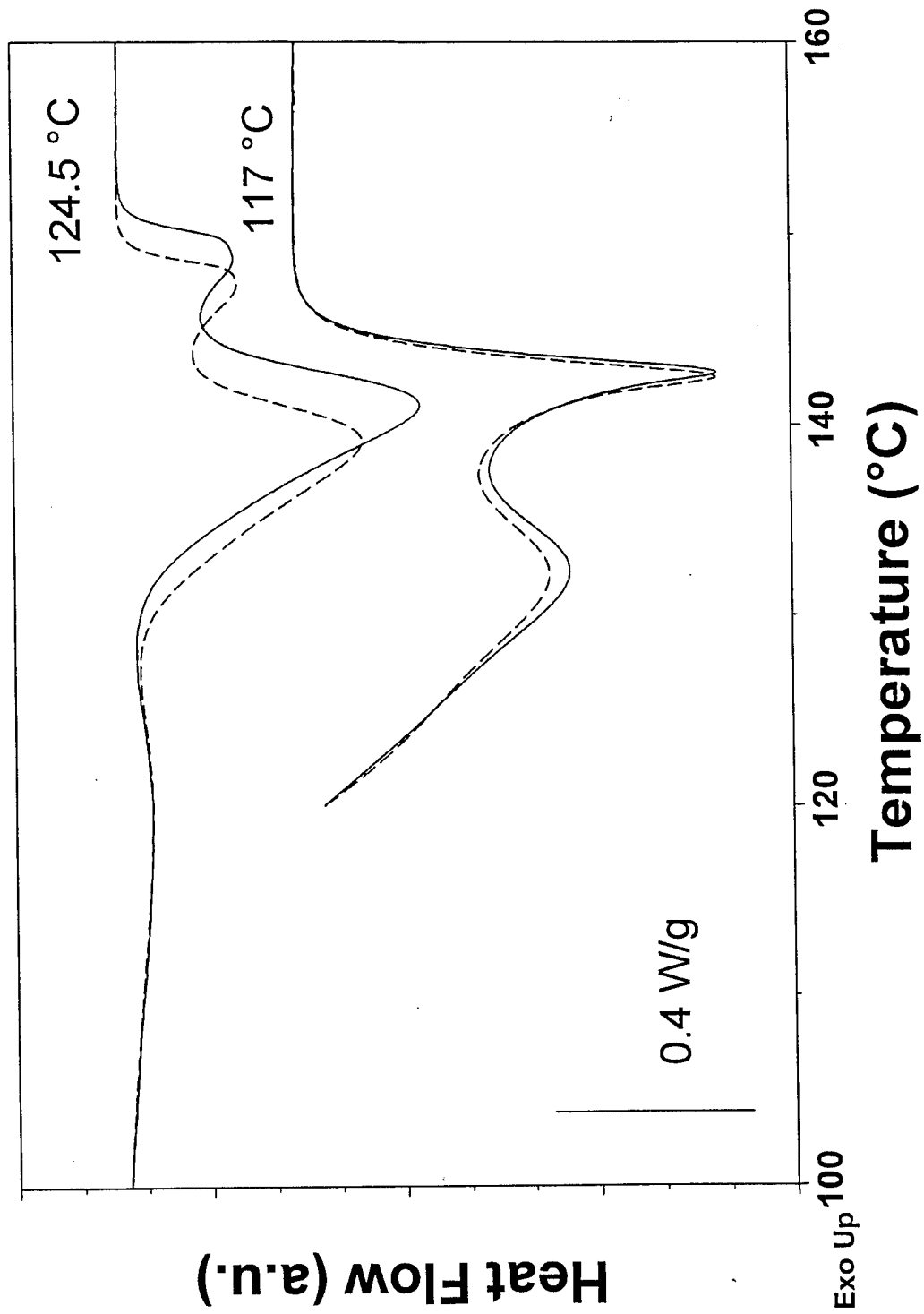


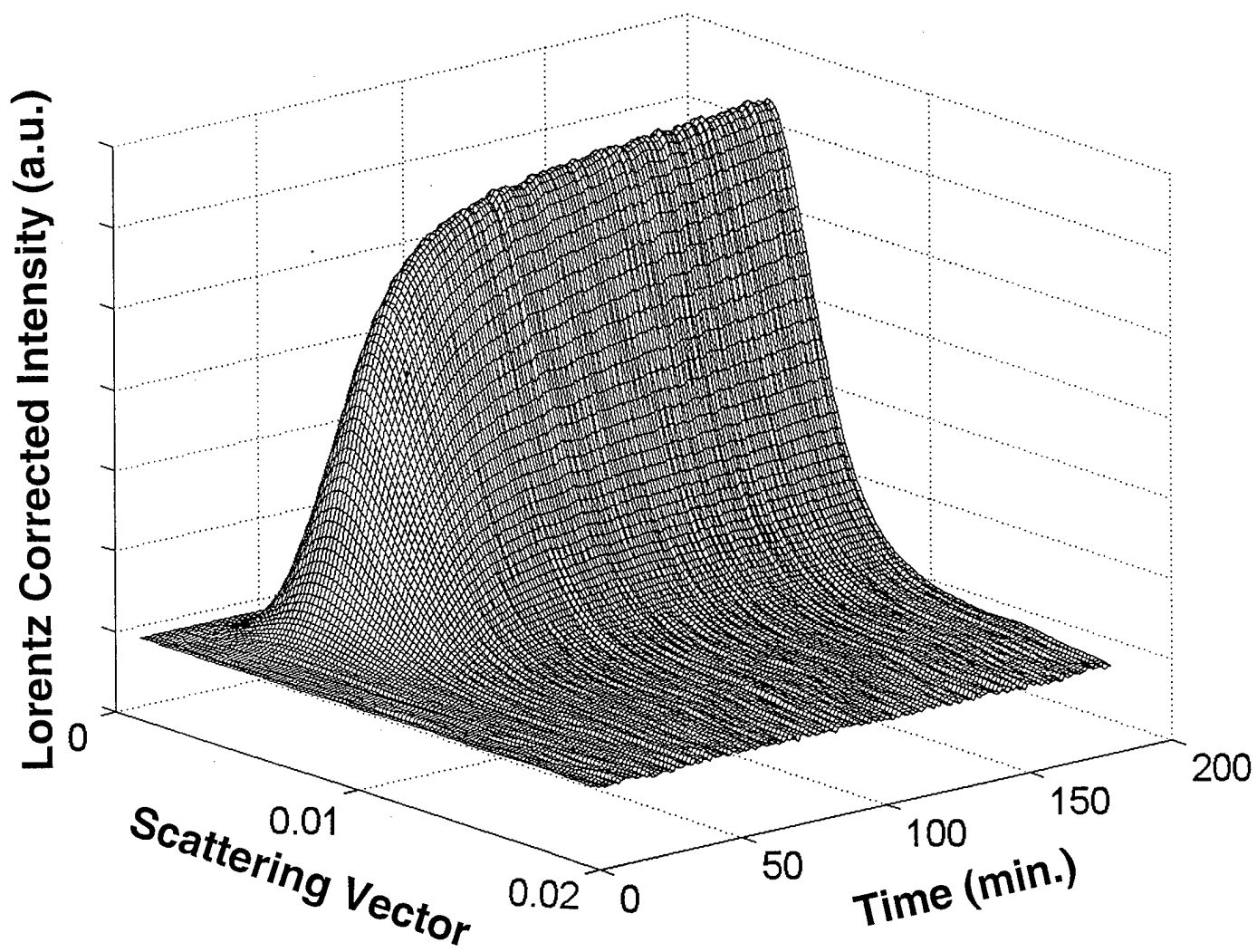
**Fig. 4** Normalized WAXS peak area,  $\eta(i)$ , from equation (2), of  $\alpha$  (solid squares) and  $\gamma$  (open circles) phase crystals of m-iPP vs. time during isothermal crystallization at: (a.) 124.5°C, and (b.) 117°C.





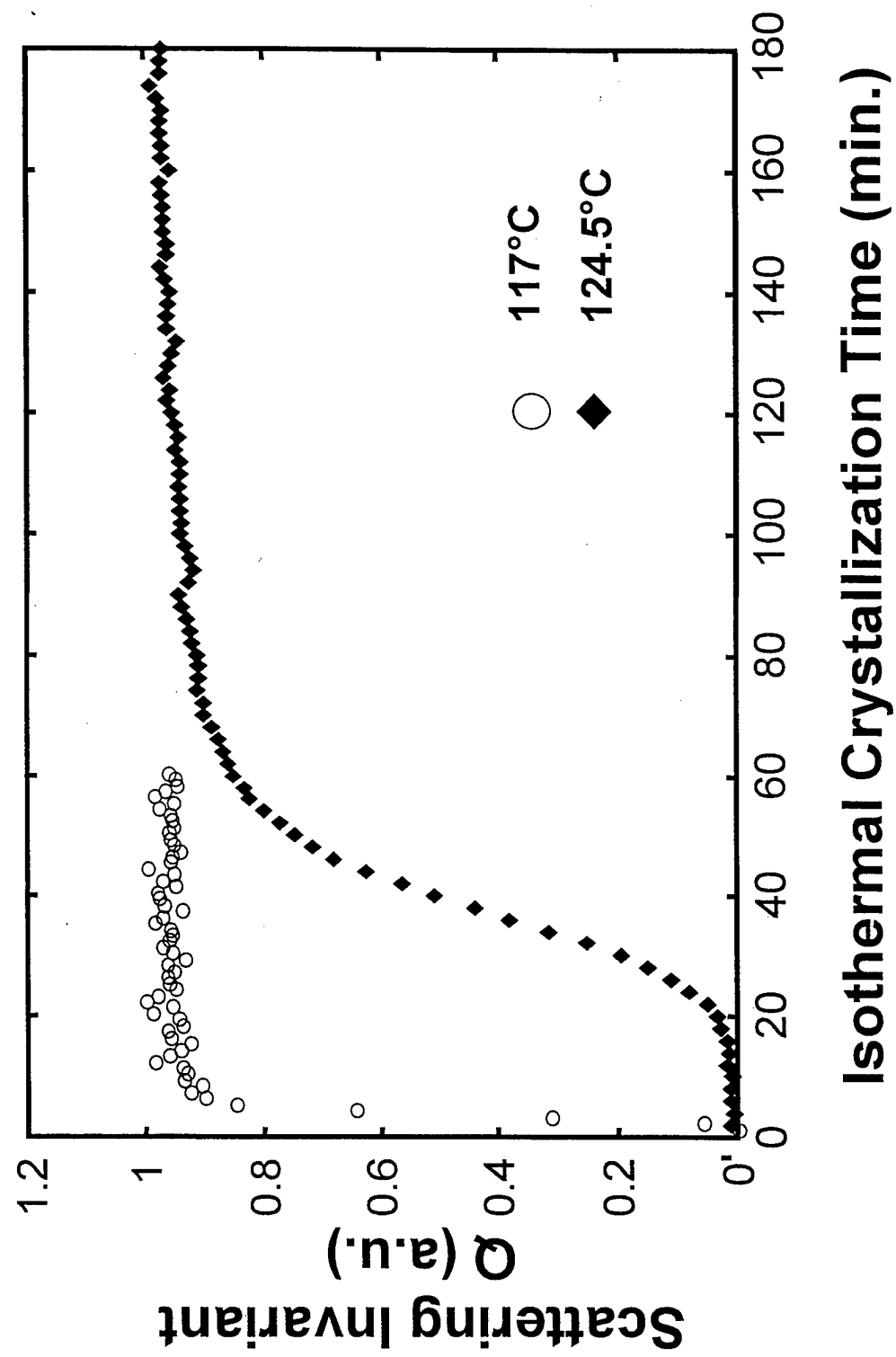
**Fig. 5** DSC exothermic heat flow of m-IPP after crystallization at 117°C for 20min(dashed line) and 40min (solid line), and at 124.5°C for 3h (dashed line) and 72h (solid line). Of the two main endotherms, the upper and lower arise from melting of  $\alpha$  and  $\gamma$  crystals, respectively.





**Fig. 6** SAXS Lorentz corrected intensity of m-iPP vs. scattering vector,  $q (=4\pi\sin\theta/\lambda)$  and vs. time during isothermal crystallization at 124.5°C.

Fig. 7 SAXS invariant,  $Q$ , of m-PP as a function of time during isothermal crystallization at 124.5°C (solid diamonds), and at 117°C (open circles).



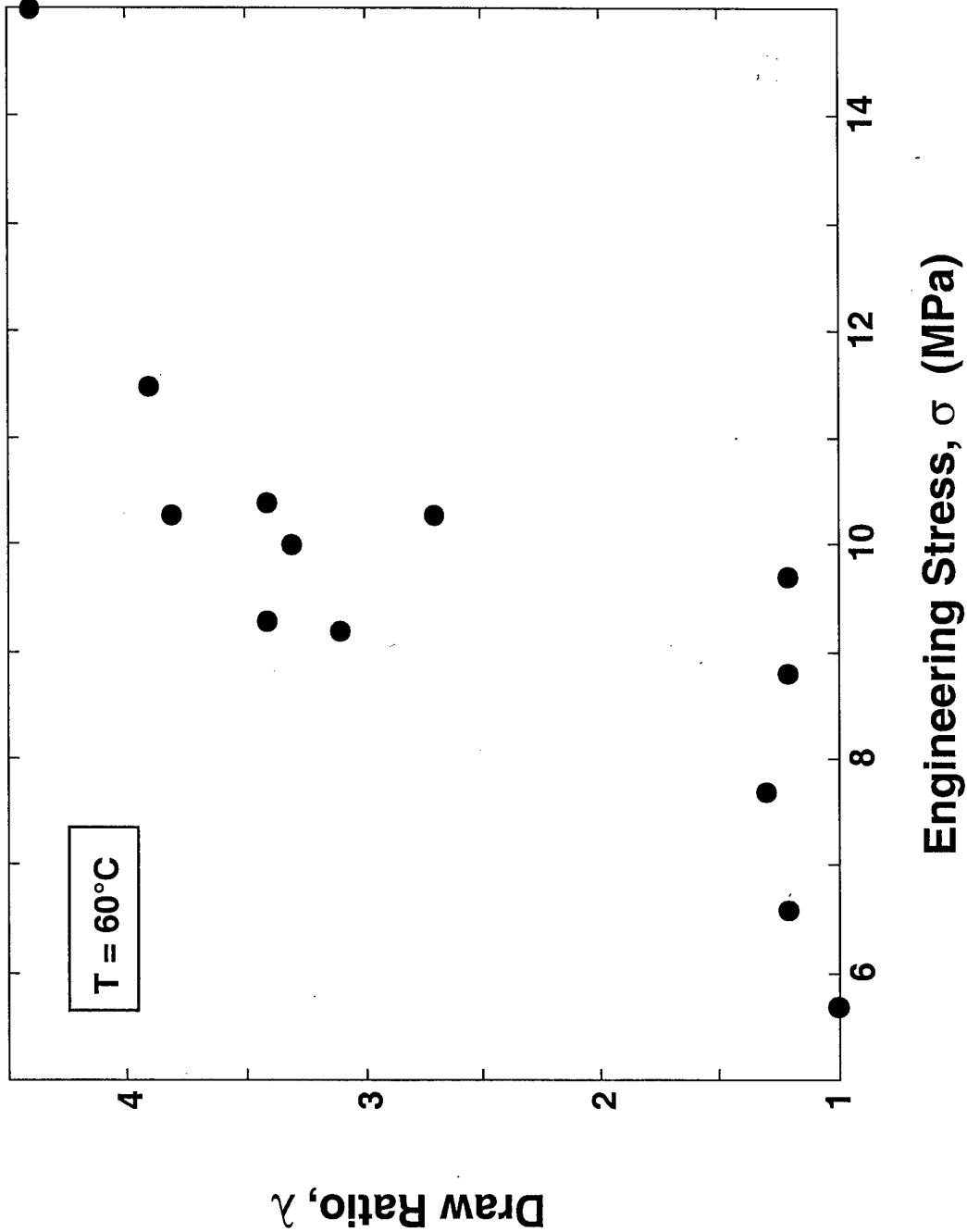


Fig. 8 Draw ratio vs. engineering stress at drawing temperature of  $60^\circ\text{C}$ .

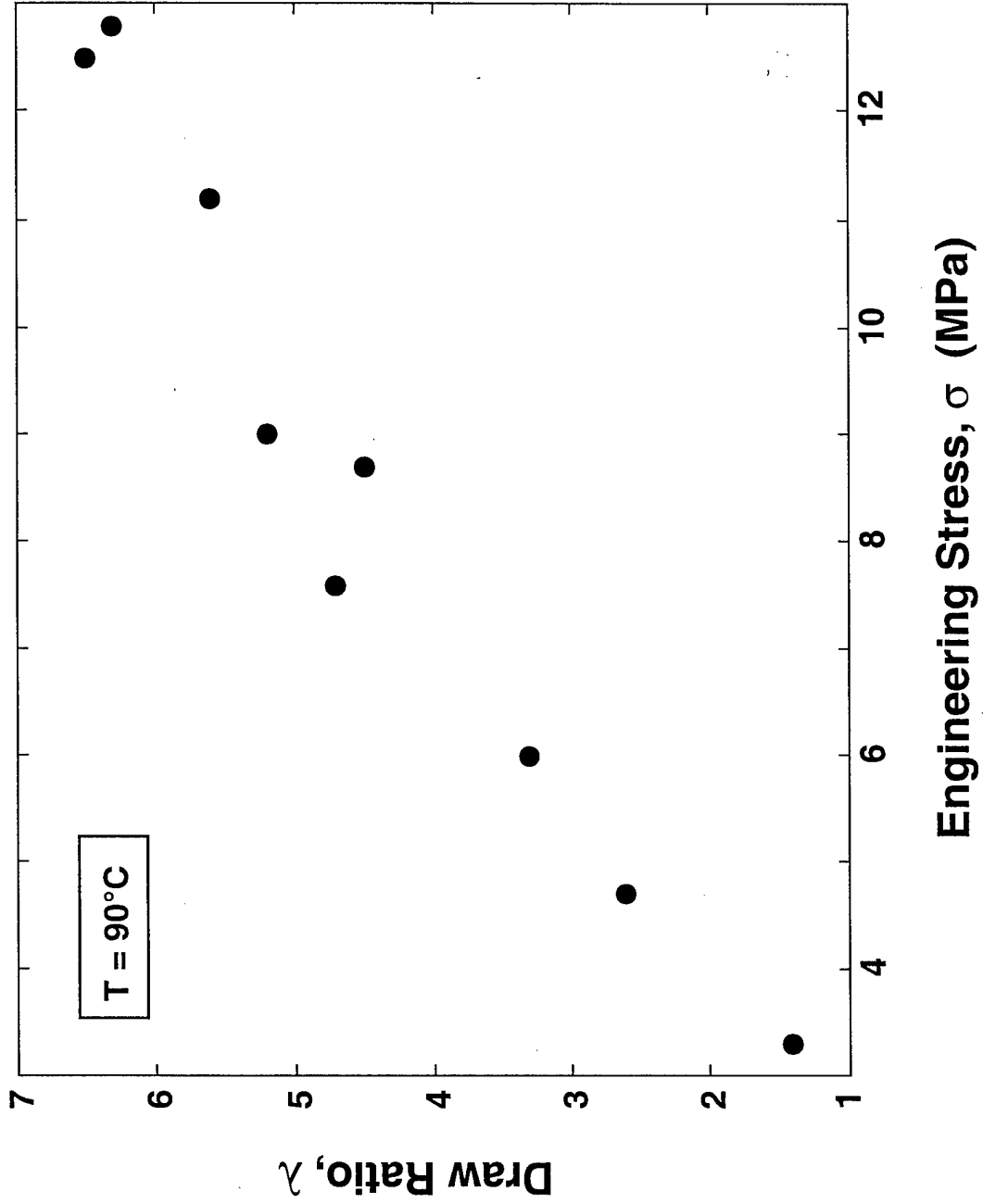
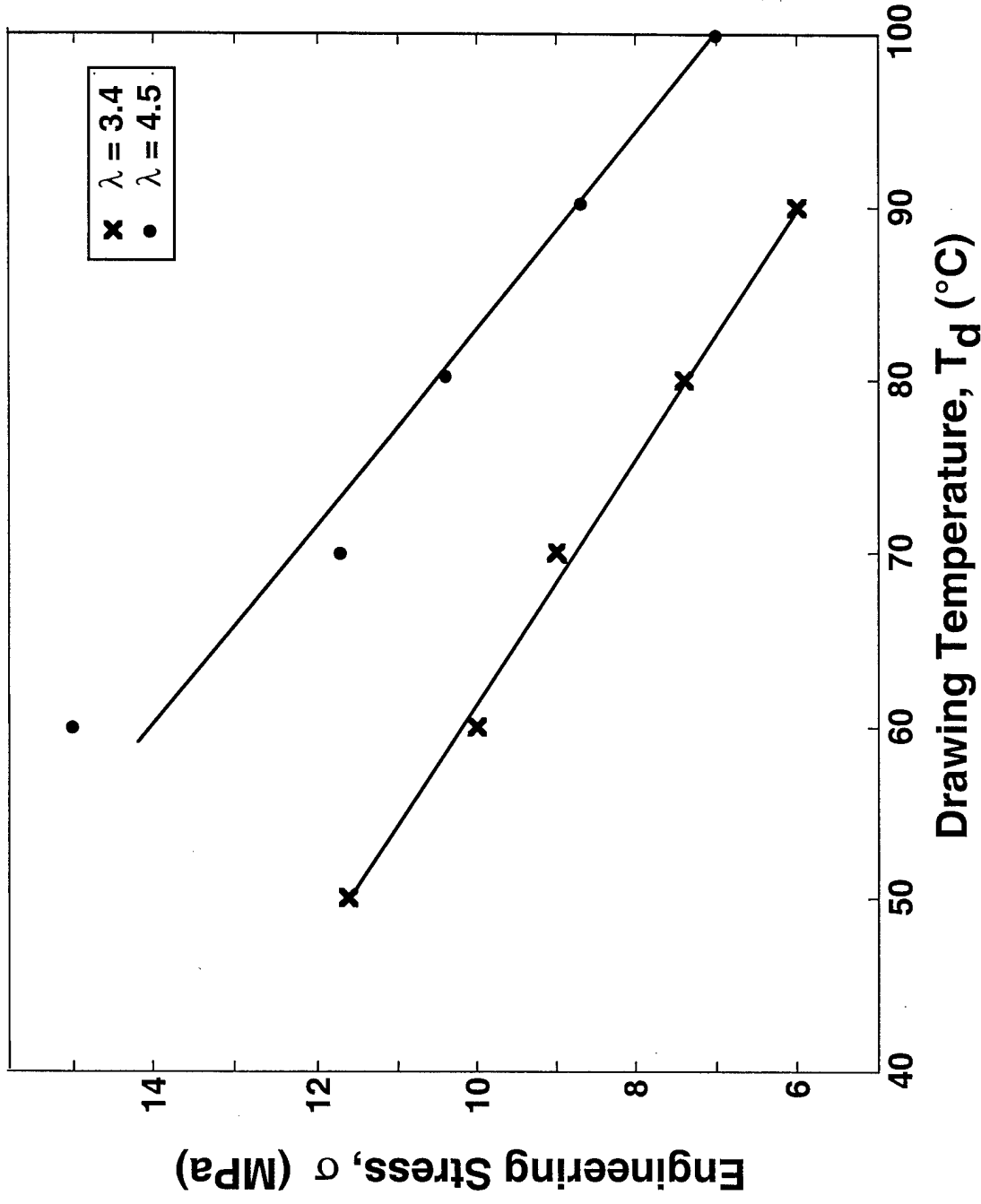
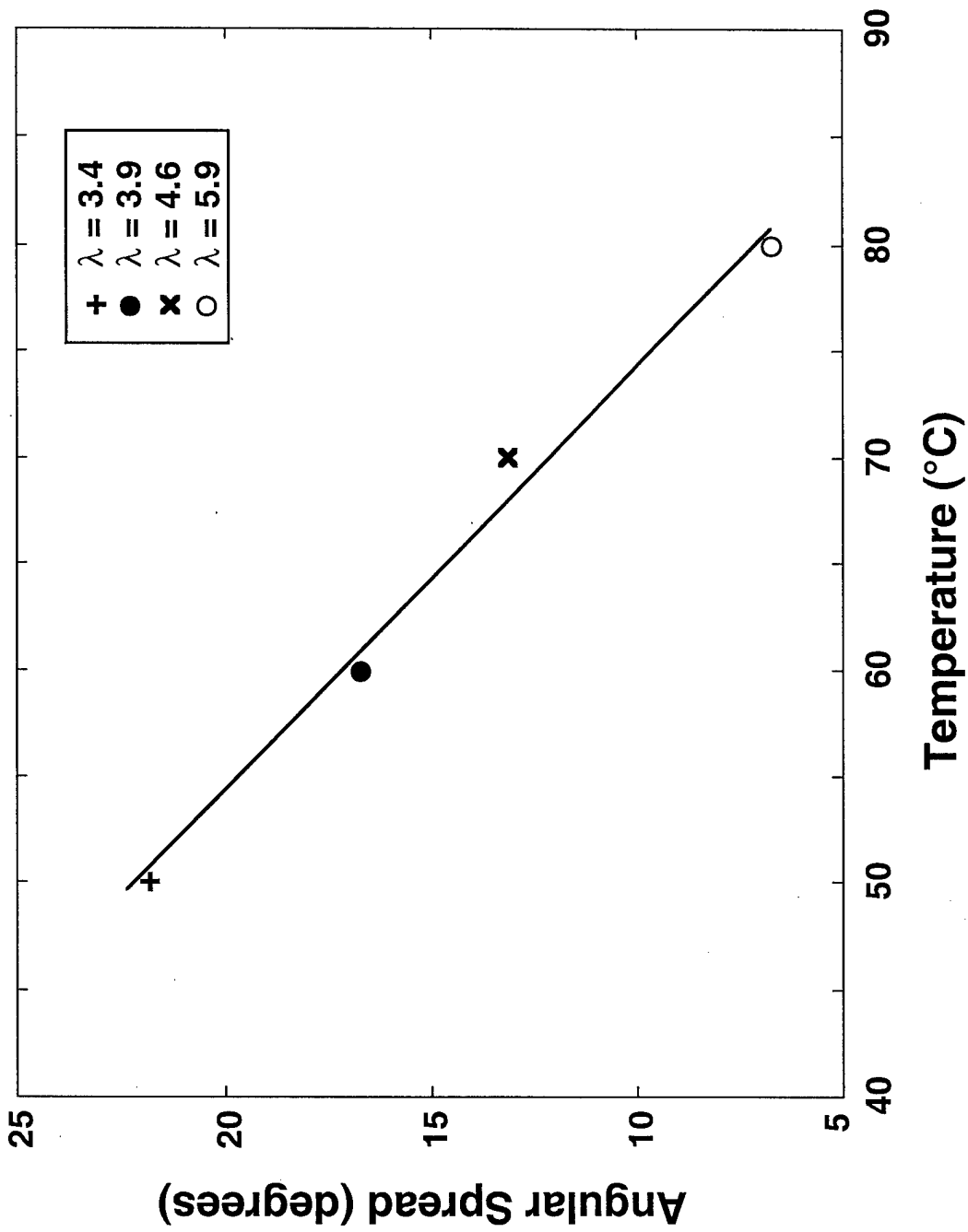


Fig. 9 Draw ratio vs. engineering stress at drawing temperature of  $90^\circ\text{C}$ .



**Fig. 10** Engineering stress vs. drawing temperature, at draw ratio of 43.4 (crosses) or 4.5 (solid circles). The lines are guides to the eye.



**Fig. 11** Angular spread of the WAXS equatorial reflections vs. drawing temperature for constant drawing stress of 11.6MPa. Different draw ratios are indicated as  $\lambda = 3.4$  (plus sign), 3.9 (solid circle), 4.6 (cross), and 5.9 (open circle).